

## THE EFFECT OF IMPREGNATION CONDITIONS ON THE SURFACE STRUCTURE OF SILICA-SUPPORTED CuO CATALYSTS

SUZY A. SELIM, HAMDY A. HASSAN, M. ABD-EL-KHALIK and RAOUF SH. MIKHAIL

*Chemistry Department, Faculty of Science, Ain Shams University, Cairo (Egypt)*

(Received 5 November 1980)

### ABSTRACT

CuO/SiO<sub>2</sub> catalysts with varying amounts of copper were prepared using meso- and microporous silica supports at pH > 10 and pH = 4.5. Structural and textural changes were followed using X-ray diffraction, TG and DTA techniques. Impregnation for periods > 10 days at high pH produces crystalline catalysts with two distinct peaks at *d*-spacings of 2.33 and 2.03 Å resulting from a surface silicate which is structurally stable up to 800°C. At copper concentrations > 5% CuO also forms. Catalysts prepared at pH = 4.5 are amorphous to X-rays in spite of the presence of CuO which may either be < 50 Å or from a surface solid solution. The copper ammine complex, if adsorbed on mesoporous silica, attains its maximum coordination number as [Cu(NH<sub>3</sub>)<sub>4</sub>(H<sub>2</sub>O)<sub>2</sub>]<sup>2+</sup>, whereas on microporous silica it loses the two water molecules as a result of pore restrictions. The surface complex releases its coordinated ammonia exothermally in the temperature range 200–400°C, whereas chemisorbed ammonia is evolved endothermally at ~280°C. Ligand water is evolved at < 200°C. An exotherm at ~545°C is observed for all catalysts, resulting from the shrinkage of the solid/void matrix which disappears upon aging. Increase of copper content to 22.7% at high pH lowered the temperature of constant weight attainment from 1000°C for the pure silica to 750°C.

### INTRODUCTION

Copper oxides supported on silica gel carriers are widely used in hydrogenation–dehydrogenation reactions [1–7], among other gas phase reactions [8,9]. The active precursor is introduced either by impregnation [10, 11] or by cation exchange [10,12–15]. The introduction of metal complexes on to silica surfaces to produce more active catalysts has been carried out by several investigators [11,16–19]. Attempts were made to study the nature of the surface structure of such catalysts [20–23] as well as their stability [22], but no general agreement as to the nature of the surface compound was achieved. Silicas with different porosities were employed [10,17, 24] for the preparation of such catalysts but the study of the mutual effect of pore structure and pH of the soaking medium on the catalyst product is lacking.

It is the aim of the present investigation to study the variation of the structural properties of the resulting CuO/SiO<sub>2</sub> catalyst upon the use of meso- and microporous silica catalysts impregnated in media of varying pH values.

## EXPERIMENTAL

*Materials*

Two types of amorphous silica gels were used as supports, Davidson 59 and 03, supplied by the Davidson Division of W.R. Grace and Company. The impregnations were achieved at two pH values, pH > 10 and pH = 4.5.

A series of samples (1A<sub>59</sub>–4A<sub>59</sub>) and (1A<sub>03</sub>–4A<sub>03</sub>) each of 10 g of the silica carrier (59 or 03) was soaked in 100 ml of Cu(NO<sub>3</sub>)<sub>2</sub> · 3 H<sub>2</sub>O (A.R.) of the required concentration and raised to the desired pH (>10) by concentrated ammonia solution with constant stirring. Each admixture was then allowed to stand for more than 10 days at room temperature, then filtered, washed with distilled water and dried at ~30°C for 24 h. The exact pH and soaking period for these catalysts are to be patented. The Cu content of each sample is shown in Table 1.

Another series of samples, 1B<sub>59</sub>, 2B<sub>59</sub>, 1B<sub>03</sub> and 2B<sub>03</sub> (Table 1), was also prepared by impregnation of silica 59 (B<sub>59</sub>) and 03 (B<sub>03</sub>) in two different concentrations of copper nitrate solutions adjusted at pH = 4.5 by HNO<sub>3</sub>. The samples were then treated as above.

*Methods*

The copper content was estimated by analysis of the impregnating solution before and after the soaking of the silica gel using EDTA titrant. The X-ray diffraction patterns were obtained using a Philips diffractometer unit,

TABLE 1

Thermogravimetric analysis data for catalysts A<sub>59</sub>, A<sub>03</sub>, B<sub>59</sub> and B<sub>03</sub>

Catalyst sample	Cu Content (%)	Total wt. loss (%)	Chemisorbed species (% per unit area)	Temp. of constant wt. (°C)
SiO <sub>2</sub> (59) at pH > 10	0.0	6.88	0.010	1000
1A <sub>59</sub>	1.0	7.39	0.009	1000
2A <sub>59</sub>	5.6	8.42	0.009	1000
3A <sub>59</sub>	13.6	8.92	0.009	800
4A <sub>59</sub>	22.7	10.58	0.008	750
SiO <sub>2</sub> (03) at pH > 10	0.0	11.25	0.009	1000
1A <sub>03</sub>	1.0	11.02	0.006	1000
2A <sub>03</sub>	5.6	11.92	0.008	975
3A <sub>03</sub>	13.6	12.45	0.013	900
4A <sub>03</sub>	22.7	12.66	0.021	850
SiO <sub>2</sub> (59) at pH = 4.5	0	6.64	0.006	950
1B <sub>59</sub>	1.0	7.16	0.115	~1000
2B <sub>59</sub>	6.7	6.85	0.010	~1000
SiO <sub>2</sub> (03) at pH = 4.5	0	21.49	0.005	950
1B <sub>03</sub>	1.0	23.07	0.006	950
2B <sub>03</sub>	6.7	24.95	0.005	950

Model PW 1010, using Zr filtered Mo radiation. The  $d$ -distances were calculated and compared with their relative intensities with data in the ASTM cards [25,26].

Thermogravimetric analyses were carried out in air (static) using a Stanton-Redcroft thermobalance type TG 750/770 connected to a BD9 two-channel automatic recorder "Kipp and Zonnen" at a heating rate of  $10^{\circ}\text{C min}^{-1}$ .

Differential thermal analysis curves were recorded using  $\alpha$ -alumina as inert standard, a programme temperature controller "Ether" transitrol type 994/2 to permit a linear rate of heating ( $12^{\circ}\text{C min}^{-1}$ ), and a Cambridge Recorder Model "B" recording the temperature difference.

## RESULTS AND DISCUSSION

### *Structural changes*

X-Ray diffraction patterns determined for the series of preparations  $A_{59}$  and  $A_{03}$  show two main peaks at  $d$ -distances of  $2.33\text{ \AA}$  and  $2.03\text{ \AA}$ , being more developed for the former. The intensity of these peaks is found to increase with increase in copper content (Fig. 1). Thermal treatment up to  $800^{\circ}\text{C}$  for 5 h does not affect these two peaks but an additional peak appears at a  $d$ -spacing of  $2.53$  (Fig. 2) which increases with increase of copper content (above 5%).

The two peaks of spacings  $2.33\text{ \AA}$  and  $2.03\text{ \AA}$  do not point to the existence of any one compound of the known copper silicate species [27,28]. It should be mentioned that a period exceeding 10 days was required for soaking at  $\text{pH} > 10$  to produce this crystallinity. It is plausible that the copper ions have interacted with the silica surface during this soaking period, first forming small nuclei which later grow in size ( $>50\text{ \AA}$ ).

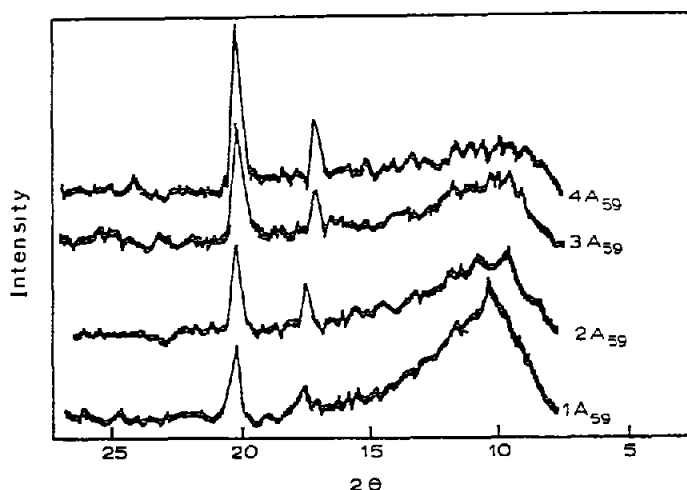


Fig. 1. X-Ray diffraction patterns for the series  $1A_{59}$ – $4A_{59}$  showing the effect of metal content.

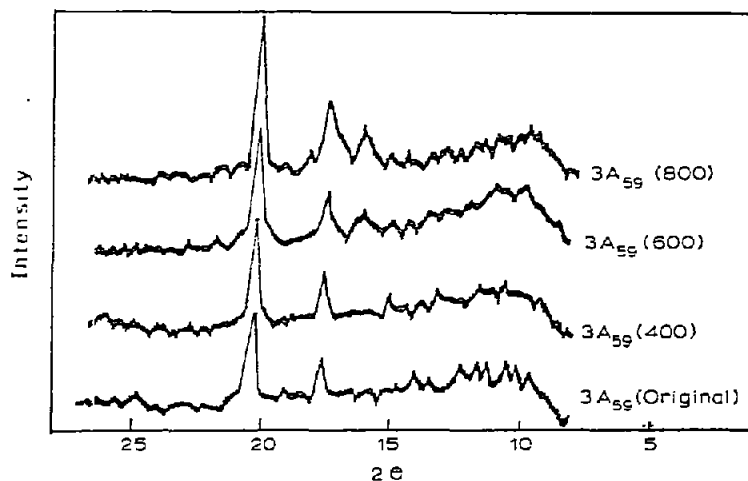
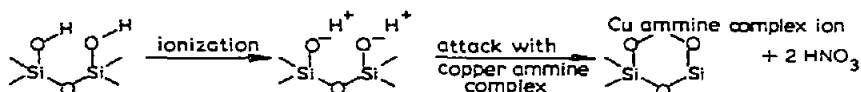


Fig. 2. X-Ray diffraction patterns for catalyst 3A<sub>59</sub> and its thermally treated products.

The peak at 2.03 is characteristic for almost all copper silicide compounds [26], yet such a compound could not possibly exist under our experimental conditions. A  $d$ -distance of 2.33 Å constitutes one of the main bands of CuO, yet the hydroxide and not the oxide would have initially formed.

From these criteria it is reasonable to assume that the silica surface is polarized [27] at such a high pH value. The divalent copper ions, surrounded by the ammonia and possibly water ligands, attack the silica surface according to the suggested scheme.

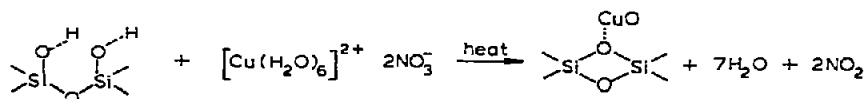


The attack of the ammine complex appears to require the existence of two adjacent hydroxyl groups on the silica surface, with the ammonia ligand being conveniently situated above the copper ions with an orientation free from any steric effects. Such an interaction would give rise to a new surface silicate structure which is thermally stable. This stability may result from the very stable configuration [28] of its six-membered ring structure.

The peak at a  $d$ -distance of 2.53 Å is characteristic for CuO, resulting from the partial hydrolysis of the copper ammine complex to the amorphous hydroxide which is converted to the oxide by heat treatment. In this case the copper ammine is believed to adsorb by electrostatic attraction on those sites which are not available to form the silicate compound. These may be the single hydroxyl sites of the silica surface which are of varying reactivity [29].

Samples 1B<sub>59</sub>, 2B<sub>59</sub>, 1B<sub>03</sub> and 2B<sub>03</sub> impregnated at pH = 4.5, as well as their thermally treated products, were amorphous to X-rays. However, it is important to note that the products heated up to 800°C for samples 2B<sub>59</sub> and 2B<sub>03</sub> (6.7% copper content) were light brown in colour, which points to the presence of CuO in the catalyst specimens. The interaction of silica surfaces with cations is only significant at pH > 7 [27] and thus the surface is

expected to be only weakly polarized at pH = 4.5. It is therefore reasonable to assume that at this low pH value the  $\text{Cu}^{2+}$  will be adsorbed on the weakly polarized surface hydroxyl groups by simple electrostatic attraction forces and will interact differently than at high pH values. This is schematically represented as



However, the amount of copper ions adsorbed is small and may also be of such small crystallite sizes ( $<50 \text{ \AA}$ ) that they are undetectable by XRD technique. X-Ray fluorescence of sample 2B<sub>59</sub> (800) showed the characteristic peak for copper located at  $2\theta = 40.03^\circ$ .

Thus the presence of copper in the solid catalysts, though not identified in the diffraction patterns, points to the existence of either very small crystallites of the adsorbed species on the surface of the support or to the possible formation of a peripheral solid solution where the copper ions have penetrated into the surface grid of the silica skeleton and become inaccessible for X-rays [22], as found for related supported systems [30–32].

#### Thermogravimetric analysis

Samples 1A<sub>59</sub>–4A<sub>59</sub> and 1A<sub>03</sub>–4A<sub>03</sub>, together with their corresponding pure silica gels, show an initial rapid loss in weight which commences at temperatures  $<100^\circ\text{C}$  and slows down at  $\sim 180^\circ\text{C}$ . Figure 3 shows the TG curves of the series 1A<sub>59</sub>–4A<sub>59</sub> and the pure soaked silica (59). This loss in weight corresponds to the loss of both adsorbed ammonia and H-bonded water which may be either attached to already adsorbed water molecules or to the surface hydroxyl groups [33] (cf. following section).

In this temperature range a greater percentage loss is observed upon the

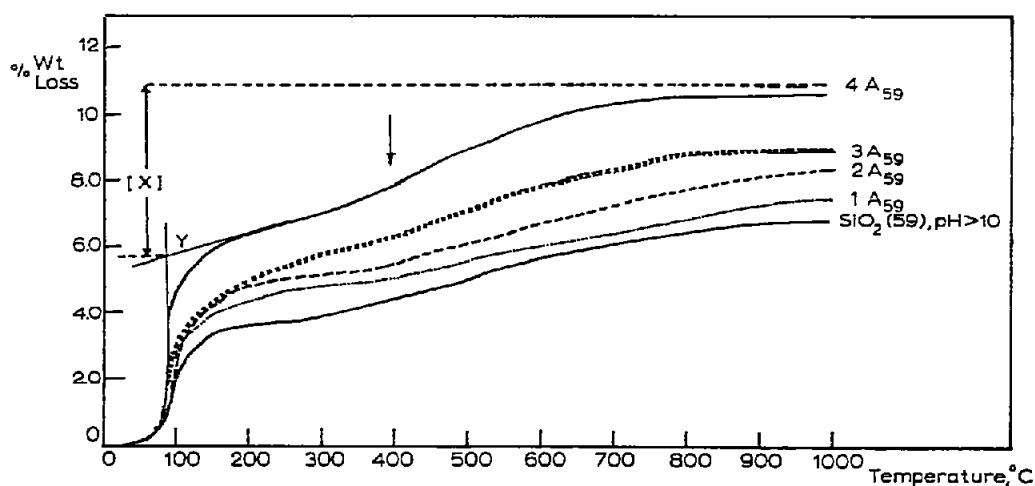


Fig. 3. Thermogravimetric curves for catalysts 1A<sub>59</sub>–4A<sub>59</sub> and the pure soaked silica (59) at pH > 10.

increase of the copper content for the catalyst series  $1A_{59}$ – $4A_{59}$ , but not for the series  $1A_{03}$ – $4A_{03}$  supported on microporous silica. As will be shown later, the surface complex supported on silica gel (59) is able to incorporate ligand water, whereas the smaller pore dimensions [34] of silica carrier (03) would hinder such a solvation taking place resulting from steric effects. This is also reflected in the difference in total percentage loss between the pure soaked silica and the corresponding catalyst, with maximum copper content being 1.41% for silica carrier (03) and 4.1% for silica carrier (59) (cf. Table 1).

A gradual loss is observed above  $250^{\circ}\text{C}$  and up to  $1000^{\circ}\text{C}$  for pure silica gels, which results from the dehydroxylation of the silanol groups besides the evolution of chemisorbed ammonia (following section). Catalysts  $1A_{59}$ – $4A_{59}$  and  $1A_{03}$ – $4A_{03}$  reproduce this increased loss in weight which forms a clear step for catalysts with the highest copper content, namely  $4A_{59}$  and  $4A_{03}$  (marked by an arrow). In this temperature range ( $\sim 400^{\circ}\text{C}$ ), the surface complex releases the ammonia ligand (see following section); also, the decomposition of the copper hydroxide present contributes to this increased loss and is significant for preparations with high copper content. A constant weight is attained at temperatures lower than  $1000^{\circ}\text{C}$  upon the increase of copper content, namely at  $750$  and  $850^{\circ}\text{C}$  for the catalysts  $4A_{59}$  and  $4A_{03}$ , respectively (Table 1, column 5). The dehydroxylation which takes place at such high temperatures ( $\sim 750$ – $1000^{\circ}\text{C}$ ) points to the difficulty of their detachment from the solid matrix, whether surface or bulk. The attainment of constant weight at lower temperatures may arise from (i) the formation of the surface complex in place of the hydroxyl groups, in which case the ammonia ligand is evolved at lower temperatures, and/or (ii) the penetration of the copper cations to the porous system upon the increase of the copper content, and this may either form a silicate complex in the pores as in (i) or simply adsorb onto any weakly polarized hydroxyl groups thus affecting the oxygen–hydrogen link and facilitating its dehydroxylation.

A comparison between the total loss of pure silica (59) and (03) (Table 1, column 3) reveals that the latter undergoes a much greater loss than the former. To differentiate whether this arises from an increase in the physically adsorbed species or not, the first plateau at  $\sim 200^{\circ}\text{C}$  is extrapolated backwards to intersect with the extended line of the region of increased weight loss at  $100$ – $150^{\circ}\text{C}$ , say at Y (Fig. 3). The difference between the total loss in weight and the value at Y would represent the percent of chemisorbed species denoted by X. The value of  $x$  so obtained is more significant if evaluated per unit area as obtained from  $\text{N}_2$  adsorption [34], and values of 0.010% and 0.009% for the two pure gels (Table 1, column 4) show a negligible difference (0.001%). This indicates that the number of hydroxyl and/or ammonia groups per unit area is the same in both gels.

Variations of X per unit specific surface area with copper content (Table 1, column 4) clearly point to differences brought about by the adsorbed species, especially for the high copper content catalysts. The amount of physically adsorbed species present in the pure soaked silica (59) ( $< 200^{\circ}\text{C}$ ) is found to be  $\sim 3.40\%$  (Fig. 3), whereas that for sample  $4A_{59}$  is  $\sim 5.75\%$ . The difference of  $\sim 2.35\%$  represents the excess physically adsorbed species, which

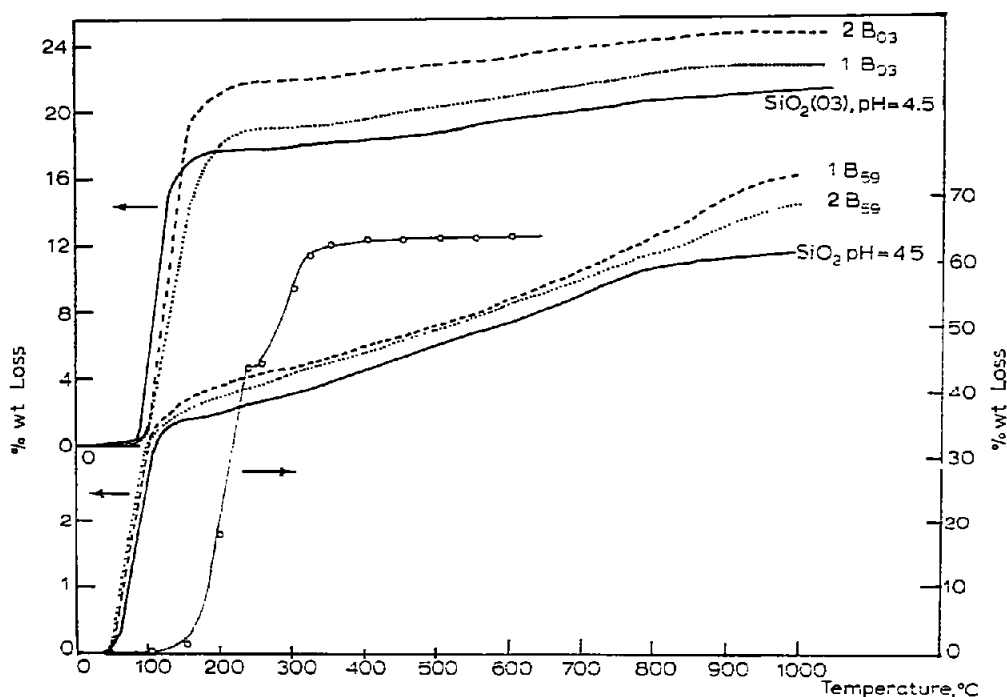


Fig. 4. Thermogravimetric curves for catalysts prepared at pH = 4.5 and also that for pure copper nitrate (right-hand scale).

is believed to be the ligand water associated with the copper complex. From Table 1, the total loss in weight for sample  $4A_{59}$  is 10.58% and therefore X (chemisorbed species) is equal to 4.88%.

As the copper ammine complex is known to have four ammonia molecules per copper atom in the aqueous phase and copper has a maximum coordination of six even in the adsorbed state [10], then from the above changes in weight loss and assuming that most of the hydroxyl groups are attacked by the copper complex in sample  $4A_{59}$ , it is realized that the excess physically adsorbed species (2.35%) is almost half of the chemisorbed species (4.88%), which suggests that the copper ammine complex is in the form  $[\text{Cu}(\text{NH}_3)_4(\text{H}_2\text{O})_2]^{2+}$  in the adsorbed state. As the coordination with ammonia is square-planar and the attachment of the water ligand is much weaker and forms an octahedron, the above configuration will only be stable if the available surface imposes no steric effects, as is the case with the mesoporous silica carrier. For microporous silica carrier (O3), however, the pores are narrower and these two water molecules are detached during the formation of the complex inside the pores, being in the form  $[\text{Cu}(\text{NH}_3)_4]^{2+}$ . This is in accordance with the TG results of sample  $4A_{O3}$  which gives almost the same percentage loss for physically adsorbed species as the corresponding pure sample.

It is important to note that as the ligand water is only weakly attached to the copper central atom in comparison to the ammonia ligand, the former will be evolved at lower temperatures, i.e. in the range for physically adsorbed species, whereas the latter will be evolved at much higher temperatures.

TG of samples  $1B_{59}$ ,  $2B_{59}$ ,  $1B_{03}$  and  $2B_{03}$  prepared at  $\text{pH} = 4.5$  shows their initial loss in weight in the same range as that of the corresponding pure soaked gels (Fig. 4), namely at  $90\text{--}200^\circ\text{C}$  and  $50\text{--}150^\circ\text{C}$  for catalysts  $B_{03}$  and  $B_{59}$ , respectively. In these solids thermal treatment at temperatures below  $200^\circ\text{C}$  causes the evolution of the adsorbed or hydrogen-bonded water originally present in the silica carrier in addition to the ligand water  $[\text{Cu}(\text{H}_2\text{O})_6]^{2+}$  which is retained by the copper in the adsorbed state [10].

The gradual loss in weight above  $200^\circ\text{C}$  results from the dehydroxylation of the catalyst carrier as well as from the decomposition of the adsorbed nitrate which occurs in the temperature range  $250\text{--}310^\circ\text{C}$  (Fig. 4). From Table 1 (column 4) it is shown that though the value of  $X$  per unit area increases upon the introduction of copper ions as for preparations  $1B_{59}$  and  $1B_{03}$ , further increase of copper content has no significant effect on  $\alpha$ . This might indicate the penetration of the precursor to the bulk of the carrier as previously suggested (XRD, section on structural changes).

It is of significance to note that the value of  $X$  per unit area is smaller at  $\text{pH} = 4.5$  than at  $\text{pH} > 10$  and also depends on the porosity of the solid material. This results from differences in the rate of decondensation [35] of silica with  $\text{pH}$ .

#### *Differential thermal analysis*

Three main endothermic effects are observed for the pure silica gels (59) and (03) soaked at  $\text{pH} > 10$  — a broad peak covering the temperature range  $\sim 80\text{--}200^\circ\text{C}$  and centered at  $\sim 110^\circ\text{C}$  and  $\sim 150^\circ\text{C}$  for the two gels, respectively, followed by a smaller endothermic peak at  $\sim 280^\circ\text{C}$  and a small plateau at  $\sim 310^\circ\text{C}$  (Figs. 5 and 6). The broad endotherm arises from the evolution of the physically adsorbed (H-bonded) ammonia [36,37] ( $<100^\circ\text{C}$ ) and water ( $100\text{--}200^\circ\text{C}$ ). The contribution of the physically adsorbed water results from two overlapping stages of evolution which should be situated at  $\sim 115^\circ\text{C}$  and  $\sim 160^\circ\text{C}$  [33] and are more distinguished for the series  $A_{03}$ .

Above  $\sim 200^\circ\text{C}$  and extending to  $\sim 400^\circ\text{C}$  is an endothermic plateau resulting from the dehydroxylation of the gel which is interrupted at  $\sim 280^\circ\text{C}$  by another endothermic effect which we believe to result from the evolution of the chemisorbed ammonia [38] attached to the ionized hydroxyl groups [27]. It is important to recall that differences in the maximum dehydroxylation temperature as observed from TG and DTA data arise from the different transfer processes in the two techniques.

At  $\sim 545^\circ\text{C}$ , a large broad exothermic peak is observed. No crystallinity is noticed from XRD and it appears that shrinkage or collapse of the solid/void matrix occurs in this temperature range at the expense of the empty voids left upon the dehydroxylation of silica. This process is accompanied by a decrease in the surface energy of the solid (decrease in specific surface area) [34] and would give rise to the observed exotherm. This exotherm disappears upon aging for periods exceeding 1 year.

The DTA thermograms of samples  $1A_{59}\text{--}4A_{59}$  (Fig. 5) and  $1A_{03}\text{--}4A_{03}$  (Fig. 6) reproduce the initial broad endotherm below  $200^\circ\text{C}$  and the two



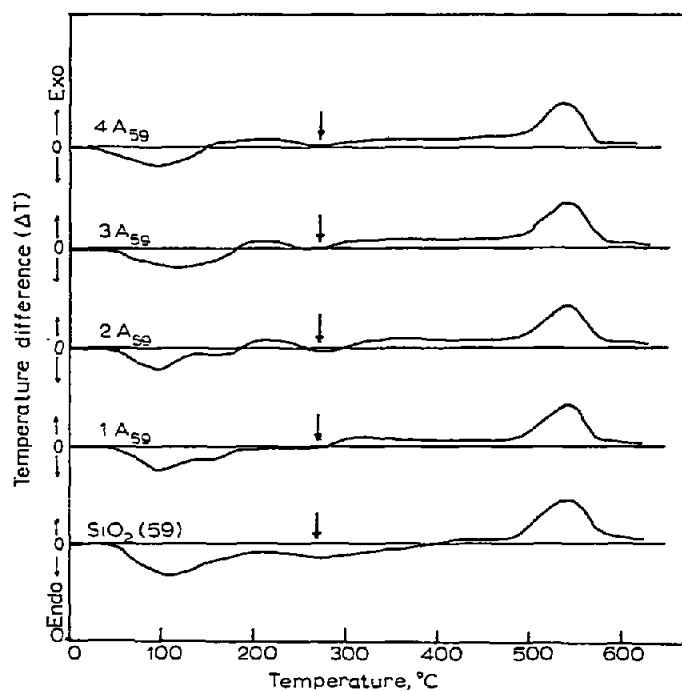


Fig. 5. Differential thermal analysis curves for pure soaked silica (59) at pH > 10 and catalysts 1A<sub>59</sub>–4A<sub>59</sub>.

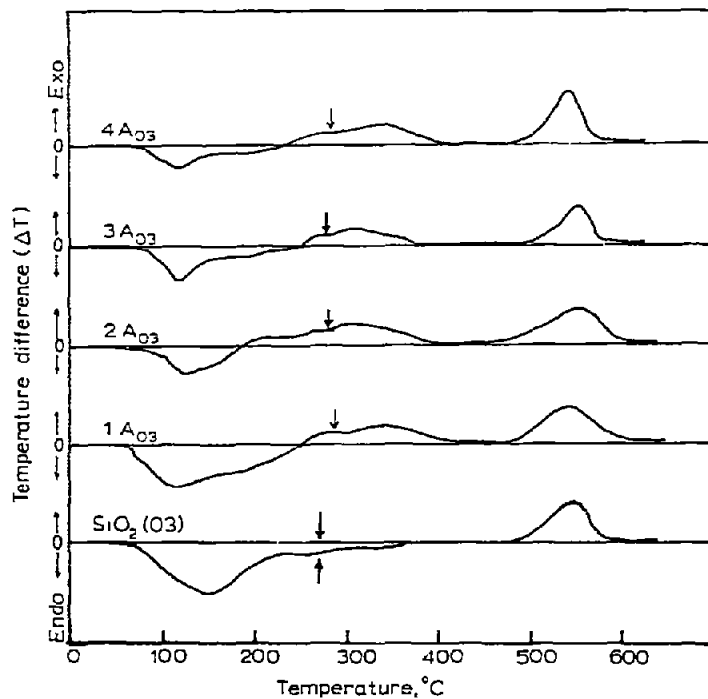


Fig. 6. Differential thermal curves for pure soaked silica (03) at pH > 10 and catalysts 1A<sub>03</sub>–4A<sub>03</sub>.

overlapping stages of water evolution become more distinguished in the presence of the copper precursor. This results from the attack of the copper ions on the surface hydroxyl groups which decreases the amount of water bound to these groups and consequently the water—water adsorbed amount. This does not appear for  $3A_{59}$  and  $4A_{59}$  due to the increased amount of water present as ligand water (section on thermogravimetric analysis). The remainder of the endothermic peaks do not appear and instead a small very broad exotherm is observed in the temperature range  $\sim 200^{\circ}\text{C}$ — $\sim 400^{\circ}\text{C}$ . This is occasionally interrupted by an endotherm (marked by an arrow) in the temperature range  $260$ — $280^{\circ}\text{C}$ , resulting from the evolution of the chemisorbed ammonia. In these preparations, the  $[\text{Cu}(\text{NH}_3)_4]^{2+} 2\text{NO}_3^-$  will attack the hydroxyl groups and will result in the disappearance of the endotherm responsible for the dehydroxylation of the surface. The decomposition of the surface complex and evolution of the ammonia ligand is exothermic, as is also found with other ammonia complexes when the anion is a nitrate [39]. The resulting peak is broad and not sharp, pointing to differences in the surface attachment of the complex which need not necessarily be energetically

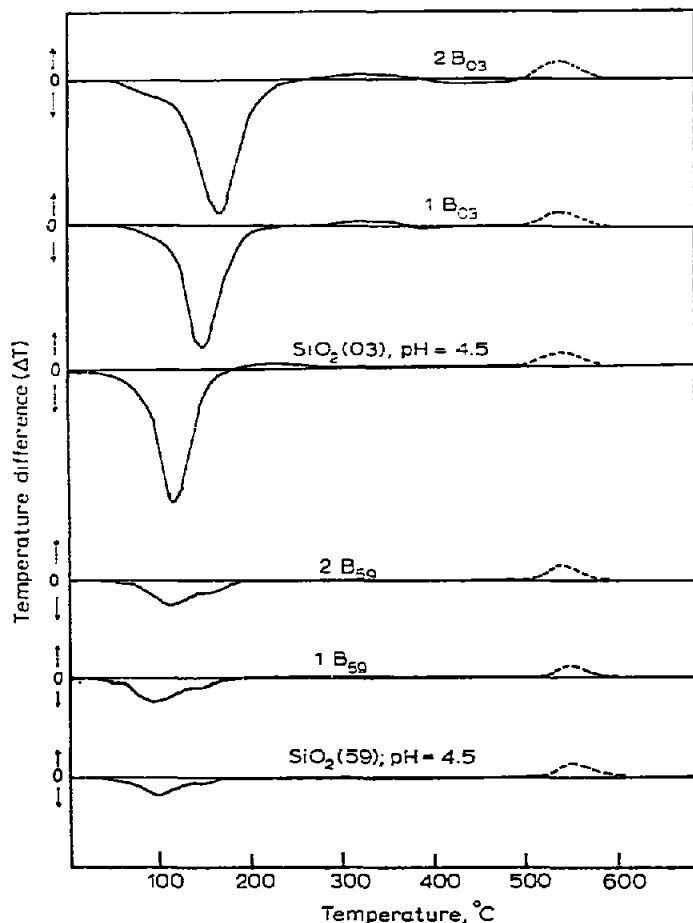


Fig. 7. Differential thermal curves for pure soaked silica gels (59) and (03) at pH = 4.5 and their corresponding impregnated catalysts.

the same. This is more pronounced for preparations  $A_{03}$  than for  $A_{59}$ , where the increased potential in the narrower pores of silica carrier (03) arising from the opposite wall effect [40] contributes to this exotherm.

DTA curves for the series of catalysts  $B_{03}$  prepared at  $\text{pH} = 4.5$  on the microporous silica support show a large endothermic peak in the temperature range  $60\text{--}220^\circ\text{C}$  similar to the corresponding soaked silica (Fig. 7). This results from the evolution of the adsorbed water, which seems to be much greater for catalyst support microporous silica (03) than mesoporous silica (59). The peak apex of this endotherm is shifted from  $115^\circ\text{C}$  for the pure soaked silica (03) to  $150^\circ\text{C}$  and  $160^\circ\text{C}$  for catalysts  $1B_{03}$  and  $2B_{03}$ , respectively. This reveals that:

(i) the adsorption of  $\text{Cu}^{2+}$  ions onto hydroxyl groups minimizes the amount of liquid-like adsorbed water evolved at  $\sim 115^\circ\text{C}$ ;

(ii) the adsorption of  $\text{Cu}^{2+}$  ions on two oppositely located hydroxyl groups at the entrances of the narrower pores hinders the evolution of the adsorbed water from these pores.

For catalyst series  $B_{59}$  (Fig. 7), this endotherm is much smaller and is split into two small endothermic effects located at  $\sim 100^\circ\text{C}$  and  $\sim 140^\circ\text{C}$ . A small exothermic plateau is observed in the range  $200\text{--}280^\circ\text{C}$  for only the pure soaked gel (03), samples  $1B_{03}$  and  $2B_{03}$  being shifted to higher temperatures upon increasing the metal content. Here the evolved water leaves behind a strained solid/void matrix which "relaxes" upon further heating. However, the presence of adsorbed  $\text{Cu}^{2+}$  cations hinders this "relaxation" slightly and delays its appearance. This phenomenon appears to be a characteristic of the micropore system.

At  $\sim 545^\circ\text{C}$  a broad exotherm is observed for all preparations, which is identical to that observed for preparations carried out at  $\text{pH} > 10$ . This also disappears upon aging.

## REFERENCES

- 1 V. Ruzicka and J. Soukup, Czech. Pat. 91,828, 1959.
- 2 I. Yasumura and T. Yoshino, *Kogyo Kagaku Zasshi*, 69(9) (1966) 1868.
- 3 K. Sambasivarao, *J. Am. Oil Chem. Soc.*, 45(3) (1968) 197.
- 4 B. Dovark and J. Pasek, *Chem. Prum.*, 18(6) (1968) 288.
- 5 W. Jerzy and Z. Ludwik, (*Zaklady Chemiczne*) "Oswiecim"; Pol. 54, 466 CCl. Bolj; 5 Jan. 1968. Appl. 15 Oct. 1965, 2pp.
- 6 W. Seaman and D. Ir. Stewart, U.S. Pat. 3,803,010, 1974 assigned to American Cyanamid Company.
- 7 Yu.A. Gorin, N.A. Rozenberg and G.F. Filatova, *Zh. Prikl. Khim.*, 39(3) (1960) 646.
- 8 M. Popl, K. Pecka, O. Weisser and J. Mostecky, *Neftekhimiya*, 9 (1969) 506.
- 9 M. Reich, W. Muller and M. Zur Hausen, U.S. Pat. 3,925,490; 1975; assigned to Chemische Werke Huls AG, Germany.
- 10 J.H. Anderson, Jr., *J. Catal.*, 28(1) (1973) 76.
- 11 T. Hidemitsu, Y. Ono and T. Keii, *J. Catal.*, 40(2) (1975) 197.
- 12 A.P. Dushina and V.B. Aleskovskii, *Zh. Obshch. Khim.*, 38(7) (1968) 1419.
- 13 K. Morikawa, T. Shirasaki and M. Okada, in: D.D. Eley, H. Pines and P.B. Weisz (Eds.), *Advances in Catalysis*. Vol. 20, Academic Press, New York, 1969, p. 87.
- 14 I. Furuoya, T. Yanagihara and T. Shirasaki, *J. Chem. Soc. Jpn., Ind. Chem. Sect.*, 72 (1969) 1346.

- 15 I. Furuoya and T. Shirasaki, *Bull. Jpn. Pet. Inst.*, 13 (1971) 78.
- 16 R.L. Burwell, Jr., R.G. Pearson, G.L. Haller, P.B. Tjok and S.P. Chock, *Inorg. Chem.*, 4 (1965) 1123.
- 17 I.P. Alekseva and A.P. Dushina, *Kolloidn. Zh.*, 31 (1968) 483.
- 18 J.W. Geus, J.M.G. Eurlings Jacobus and N.V. Stamicarbob, *Ger. Offen.*, 1,963,827, 1970; *Neth. Appl.* 20 Dec., 1968.
- 19 A.A. Denisov and B.A. Zhidkov, *Katal.*, 9 (1972) 103.
- 20 V.M. Vst'Yautsev, L.P. Sudakova and A.F. Bessonov, *Zh. Neorg. Khim.*, 11(5) (1966) 1177.
- 21 B.J. Hathaway and C. Lewis, *J. Chem. Soc. A*, (15) (1964) 2295.
- 22 F.N. Khasanov, E.S. Svetsitskii and V.N. Vorobev, in A. Abdukadyrov (Ed.), 3rd *Mater. Resp. Nauchnotekh.*, Kauf Molodykh U. Ch. Pereab. Nefti Neftekhim, Sredne-aziat. Nauchno-Issled, Inst. Noftepereab. Prom-Sti, Tashkent, U.S.S.R., 1976, Vol. 2 p. 34.
- 23 A.V. Bogdanov, V.A. Shvets and V.B. Kazanskii, *Kinet. Katal.*, 15(1) (1974) 176.
- 24 Agromomov, V.I.A.E.; and Li-Tang Ling, *Vestn. Mosk. Univ., Ser. Khim.*, 16(6) (1961) 53.
- 25 J.V. Smith (Ed.), *X-ray Powder Data File and Index To X-ray Data File*, Am. Soc. Testing Mater., Philadelphia, 1961.
- 26 *Powder Diffraction File, ASTM Alphabetical Index of Inorganic Compounds*, Published by the International Center for diffraction data, 1978; Swathmore, PA 19081, U.S.A.
- 27 J.P. Brunelle, *Pure Appl. Chem.*, 50 (1978) 9.
- 28 D. Dollimore, in R.C. MacKenzie (Ed.), *Differential Thermal Analysis, Vol. 1*, Academic Press, London, New York, 1970, p. 443.
- 29 J.B. Peri, *J. Catal.*, 41 (1976) 227.
- 30 K.P. Zhdanova, *Kinet. Katal.*, 9 (1968) 853.
- 31 E.D. Pierron, J.A. Rashkin and J.F. Roth, *J. Catal.*, 9 (1967) 38.
- 32 S.A. Hassan, M.A. Abd-El-Khalik and H.A. Hassan, *J. Catal.*, 52 (1978) 261.
- 33 S.A. Selim, S.A. Hanafi and M. Ismail, in preparation.
- 34 H.A. Hassan, Ph.D. Thesis, Ain Shams University, Cairo, Egypt 1980.
- 35 C. Okkerse, in B.G. Linsen (Ed.), *Physical and Chemical Aspects of Adsorbents and Catalysts*, Academic Press, New York, 1970.
- 36 N.W. Cant and L.M. Little, *Can. J. Chem.*, 42 (1964) 802.
- 37 M. Folman and D.J.C. Yates, *Proc. R. Soc. London, Ser. A*, 246 (1958) 32.
- 38 R.P. Eischens and W.A. Pliskin, *Advances in Catalysis, Vol. X*, Academic Press, New York, 1958.
- 39 W.W. Wendlandt and I.P. Smith, *J. Inorg. Nucl. Chem.*, 26 (1964) 445.
- 40 R.Sh. Mikhail, Sh. Nashed, and A.M. Khalil, *Discuss. Faraday Soc.*, 52 (1971) 187.